JOURNAL OF CATALYSIS 150, 335–344 (1994)

Infrared Spectroscopic Studies of CO Adsorption on Rhodium Supported by SiO_2, Al_2O_3, and TiO_2

Sabine Trautmann and Manfred Baerns[1]

Lehrstuhl für Technische Chemie, Ruhr-Universität Bochum, D-44780 Bochum, Germany

Received September 8, 1993; revised June 27, 1994

CO adsorption on Rh (0.5 wt%) supported by SiO_2, Al_2O_3, and TiO_2 was studied by DRIFT spectroscopy at 296 K and atmospheric pressure. A support effect on the particle size distribution was evident by dominant dicarbonyl species on Rh/Al_2O_3 and Rh/TiO_2, characteristic for CO adsorption on dispersed clusters, while significant proportions of linear- and bridged-bonded CO, ascribed to CO adsorbed on crystalline rhodium, were observed on Rh/SiO_2. Adsorption and desorption of CO was nondissociative on Rh/SiO_2, while on Rh/Al_2O_3 and Rh/TiO_2 CO dissociation occurred at 296 K. CO desorption at 296 K was reductive, which led to irreversible agglomeration of rhodium clusters; in thermal CO desorption (up to 500 K), this process was strongly enhanced. © 1994 Academic Press, Inc.

INTRODUCTION

The interaction between CO and supported rhodium is known to produce three distinct adsorption modes, viz., dicarbonyl, linear-bonded CO, and bridged-bonded CO, as demonstrated by Yang and Garland (1) in their early and very detailed IR work in CO adsorption on Rh/Al_2O_3. While Rh^0 clusters bind CO in linear and bridged forms, singly charged Rh^+ ions are considered to be the adsorption sites responsible for the dicarbonyl complex. For the existence of Rh^+ the dissociation of CO followed by oxidation of Rh^0 with the adsorbed oxygen formed (2–5) as well as the oxidation of Rh^0 by surface hydroxyl groups has been discussed (6–12). Since the dicarbonyl complex is dominant on well-dispersed rhodium while linear-bonded and bridged-bonded CO species appear progressively with increasing metal loading, CO may be used as an indicator for structural changes. CO adsorption on supported rhodium occurs by two mechanisms: (i) at low temperatures (ca. 300 K), the oxidative disruption of Rh^0 leads to isolated Rh^+ clusters; (ii) at higher temperatures, Rh^0 crystallites are formed by reductive agglomeration of Rh^+. These findings are supported by EXAFS and ESR studies (2, 6, 13, 14). Recently, Solymosi and Knözinger (15) investigated this phenomenon on a Rh(1 wt%)/Al_2O_3 catalyst at temperatures ranging from 85 to 573 K by IR spectroscopy. They found that the oxidative disruption of Rh^0, i.e., the formation of dicarbonyls, starts at temperatures as low as 150 K, while the reductive agglomeration of Rh^+, which was evident by a strong increase in intensity of bands due to linear-bonded and bridged-bonded CO, begins at 473 K. For rhodium catalysts showing a similar metal loading, the nature of the support was proven to influence the particle size distribution; thus, dicarbonyls are more favored on Rh/Al_2O_3 than on Rh/SiO_2 (16–18). As a possible explanation for preferred dicarbonyls on Rh/Al_2O_3, a stronger oxidation potential of OH groups to produce Rh^+ has been proposed. Buchanan *et al.* (6), who studied CO adsorption on Rh/TiO_2 by IR spectroscopy, suggested that dicarbonyls should also be suppressed on Rh/TiO_2; i.e., oxidation potentials of OH groups on TiO_2 should be lower than those on Al_2O_3. This conclusion was based on comparison of their IR results with literature data for similarly loaded Rh/Al_2O_3 catalysts (7).

The aim of the present study was to obtain a deeper insight into the nature of interaction between CO and rhodium on different supports, i.e., SiO_2, Al_2O_3, and TiO_2. Particular attention was paid to the influence of the support on the adsorption state of CO and to the desorption of CO, which is discussed in terms of structural changes of the deposited metal.

EXPERIMENTAL

1. Catalyst Preparation

The SiO_2 (300 $m^2\ g^{-1}$), Al_2O_3 (100 $m^2\ g^{-1}$), and TiO_2 (50 $m^2\ g^{-1}$) supported rhodium catalysts were prepared by Ioannides and Verykios (19) by the method of incipient-wetness impregnation using $RhCl_3 \cdot 3H_2O$ as the precursor compound for the metal. The received catalysts were pretreated in a flow of N_2 (50 $cm^3\ min^{-1}$) at 473 K for 1 h and subsequently reduced in flowing H_2 (50 $cm^3\ min^{-1}$) at 473 K for 1 h and for another hour at 523 K. The metal

[1] To whom correspondence should be addressed.

0021-9517/94 $6.00

loading amounted to 0.5 wt%; the metal dispersion was determined by static equilibrium adsorption of H_2 at 298 K assuming dissociative H_2 adsorption and 1-to-1 stoichiometry. The H : Rh ratios (atoms of hydrogen adsorbed per Rh atom) were 1.29 for Rh/SiO_2, 1.00 for Rh/Al_2O_3, and 0.70 for Rh/TiO_2, indicating that rhodium was highly dispersed.

2. Infrared Studies

For infrared studies a Perkin–Elmer 1710 spectrometer was used to which a diffuse reflectance accessory (Spectra Tech, Model 0030-103) was attached. Spectra were based on 50 scans with a resolution of 4 cm^{-1}; thus, one spectrum took 3.5 min. The recorded diffuse reflectance spectra were transformed to Kubelka–Munk units; KBr served as reference. The spectra presented in this paper show absorptions of the adsorbate only; i.e., background absorption of the catalysts was subtracted from the original spectra.

The gases were controlled by mass flow meters; N_2 (99.999%), H_2 (99.999%), and CO (10% in He) were further purified by Oxisorb for removal of traces of O_2 and H_2O.

The measurements were performed under atmospheric pressure. Prior to CO adsorption the prereduced catalysts (see above) were treated *in situ* in a flow of H_2 (5 cm^3 min^{-1}) diluted by N_2 (10 cm^3 min^{-1}) at 473 K for 2 h. After reduction, the temperature was further held at 473 K for 30 min while the catalysts were purged with N_2 (10 cm^3 min^{-1}). For CO adsorption, the catalysts were first cooled to 296 K under the flow of N_2, then pulses of CO (0.025 cm^3) were repeatedly injected into the inert carrier stream until chemisorption was complete, i.e., until no further change in adsorbate structures was observed. CO desorption in flowing N_2 was investigated (a) at 296 K and (b) by increasing the temperature in 25-K steps. Spectra were recorded at 296 K in time intervals of 30 min, and in thermal desorption at every temperature step. Since constant temperature was established within a few seconds, the time under flowing N_2 at each temperature was about 3.5 min, which corresponds to the time for scanning one spectrum. After desorption, the catalysts were re-exposed to CO at 296 K to elucidate structural changes which may have occurred during CO desorption from the metal surface.

RESULTS AND DISCUSSION

IR results for adsorption, desorption, and re-adsorption of CO on rhodium catalysts are presented separately for the various supports used, namely, SiO_2, Al_2O_3, and TiO_2. Since CO spectra on Rh/SiO_2 were strongly disturbed by a low signal-to-noise ratio, due to strong absorption of SiO_2, thermal CO desorption as well as re-adsorption studies were performed on only Rh/Al_2O_3 and Rh/TiO_2 to obtain reliable conclusions.

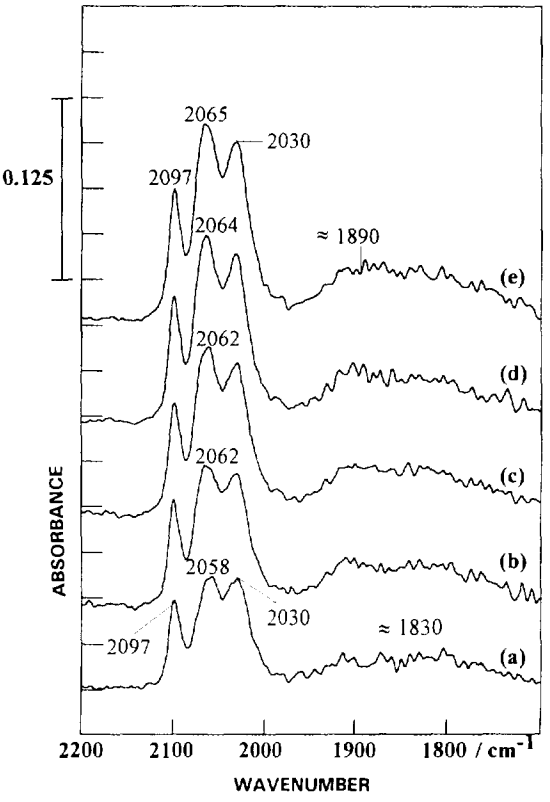

FIG. 1. Infrared spectra of CO adsorbed on Rh(0.5 wt%)/SiO_2 after exposure to (a) 1, (b) 2, (c) 3, (d) 6, and (e) 10 pulses of CO (0.025 cm^3) at 296 K.

1. CO Adsorption at 296 K

Rh/SiO_2. Results are shown in Fig. 1. After the first CO pulse, bands of similar intensities at 2097, 2058, and 2030 cm^{-1}, as well as a broad absorption centred at ca. 1830 cm^{-1} were detected. With increasing surface coverage, the bands at 2097 and 2030 cm^{-1} developed at constant positions, the other bands shifted to higher wavenumbers, i.e., 2058 → 2065 cm^{-1} and 1830 → 1890 cm^{-1}, respectively. In accordance with literature data (1), CO frequencies at 2097 and 2030 cm^{-1} are assigned to the symmetrical and asymmetrical stretching vibration of a dicarbonyl complex on Rh^+. The development of the bands at constant positions demonstrates that the adsorption sites are spatially isolated, i.e., there are dispersed clusters, since close proximity of adsorbed CO molecules should result in dipolar coupling and hence to a shift to higher wavenumbers as surface coverage increases. Bands which shift to higher wavenumbers are ascribed to CO adsorption on crystalline Rh^0: at complete CO chemisorption, the band at 2065 cm^{-1} represents the linear-

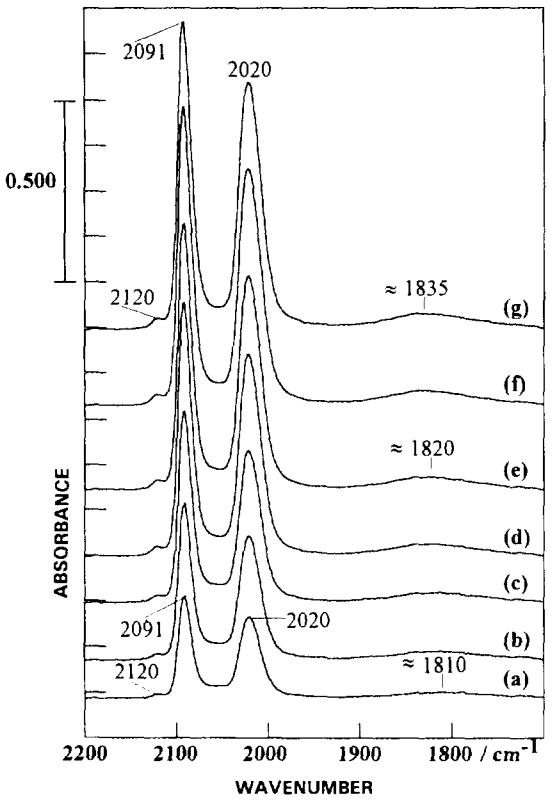

FIG. 2. Infrared spectra of CO adsorbed on Rh(0.5 wt%)/Al_2O_3 after exposure to (a) 1, (b) 2, (c) 3, (d) 6, (e) 8, (f) 13, and (g) 20 pulses of CO (0.025 cm^3) at 296 K.

bonded CO mode, while the broad absorption at ca. 1890 cm^{-1} is due to bridged-bonded CO surface species.

Rh/Al_2O_3. CO adsorption on Rh/Al_2O_3 led to two strong dicarbonyl bands at 2091 and 2020 cm^{-1} (see Fig. 2). While a weak and broad absorption of bridged-bonded CO on Rh^0 appeared first at 1810 cm^{-1} and shifted to 1835 cm^{-1}, linear-bonded CO on Rh^0 was not formed. The weak band at 2120 cm^{-1} corresponds to linear-bonded CO on Rh^{2+} typical for oxidized rhodium catalysts (20), which in turn indicates that adsorbed oxygen exists on the metal surface. Therefore, the conclusion is drawn that CO partly dissociates on Rh/Al_2O_3 at 296 K.

Rh/TiO_2. The dominant spectral feature, similarly to Rh/Al_2O_3, consisted of strong dicarbonyl bands which, however, unexpectedly shifted with CO coverage, i.e., 2097 → 2100 cm^{-1} and 2030 → 2034 cm^{-1}, respectively (see Fig. 3). While a weak and broad absorption of bridged-bonded CO on Rh^0 developed at ca. 1830 cm^{-1} (not shown in Fig. 3), the band of linear-bonded CO on Rh^0 was again absent. Additional bands were obvious above 2100 cm^{-1}, i.e., in the range of CO adsorbed on oxidized rhodium: the CO frequency at 2135 cm^{-1} is assigned to linear-bonded CO on Rh^{2+}, the band at 2145 cm^{-1}, visible at low surface coverage only, to linear-bonded CO on Rh^{3+} (21). For initial exposure to CO, another band was seen at 2017 cm^{-1}; from this position, bridged-bonded CO on Rh^+ may be postulated according to Rice *et al.* (21). The presence of this band also explains the shift observed for the low-frequency dicarbonyl band (2030 → 2034 cm^{-1}) by their superimposition. For similar band shifts as detected for the high-frequency dicarbonyl band (2097 → 2100 cm^{-1}), a superimposition with a band due to linear-bonded CO on Rh^+ has been proposed (21).

Results for Rh/TiO_2 strongly imply that as with Rh/Al_2O_3 adsorption of CO is dissociative at 296 K, which may be derived by the appearance of bands above 2100 cm^{-1} for CO adsorbed on $Rh^{>1+}$. Although great care has been taken in homogenizing the catalysts, adsorbate structures were found to differ for various Rh/TiO_2 samples. To illustrate this, Fig. 4 shows spectra recorded for two Rh/TiO_2 samples, i.e., sample 1 (the same as Fig. 3) and sample 2. While on sample 1 bands were obtained at 2135, 2145, and 2017 cm^{-1} (for the latter ones remarkable at low surface coverage only; see Fig. 3) for linear-bonded CO on Rh^{2+} and Rh^{3+}, and for bridged-bonded CO on Rh^+, respectively, these species were not produced on sample 2. The dicarbonyl bands were less intense on sam-

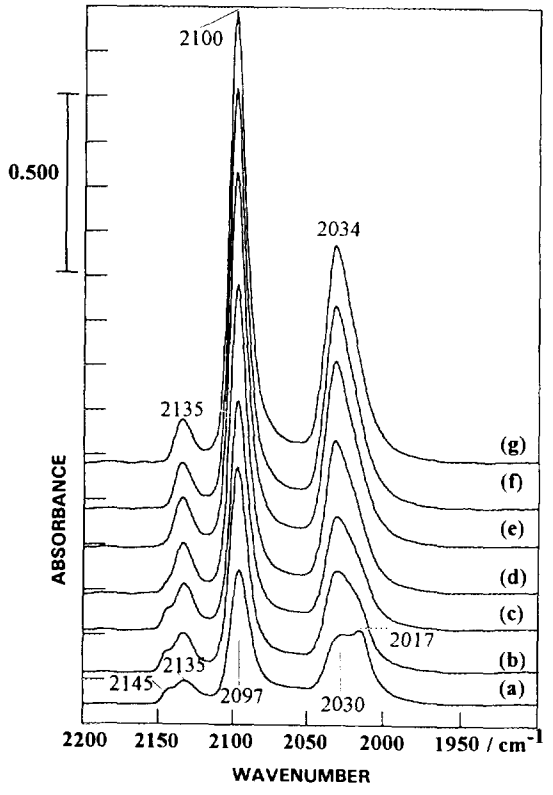

FIG. 3. Infrared spectra of CO adsorbed on Rh(0.5 wt%)/TiO_2 (sample 1) after exposure to (a) 1, (b) 2, (c) 3, (d) 6, (e) 10, (f) 15, and (g) 20 pulses of CO (0.025 cm^3) at 296 K.

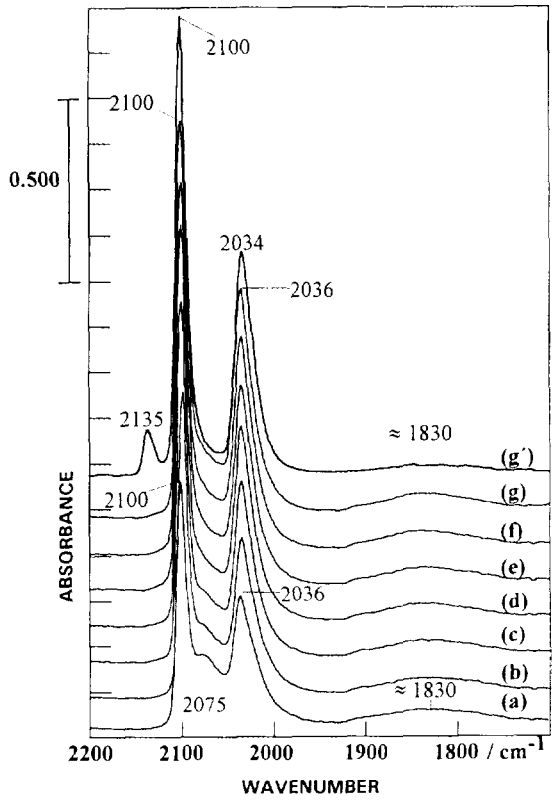

FIG. 4. Infrared spectra of CO adsorbed on Rh(0.5 wt%)/TiO_2 (sample 2) after exposure to (a) 1, (b) 2, (c) 3, (d) 6, (e) 10, (f) 15, and (g) 20 pulses of CO (0.025 cm^3) at 296 K; (g') the same as Fig. 3g.

ple 2; slight shifts as for sample 1 (see Fig. 3), which had been attributed to superimposition with absorptions of linear- and bridged-bonded CO on Rh^+, were not observed with increasing surface coverage. The band intensity of the bridged-bonded CO on Rh^0 at ca. 1830 cm^{-1} was stronger for sample 2; in addition, a resolved band of linear-bonded CO on Rh^0 was seen at 2075 cm^{-1} for initial exposure to CO. All these findings agree with a lower oxidation state of rhodium on sample 2 compared to sample 1, i.e., with CO dissociation which only occurred on sample 1; besides the above listed bands for CO linear-bonded on Rh^{3+} and Rh^{2+} or bridged-bonded on Rh^+, it is well known from the literature (22) that adsorbed oxygen on rhodium catalysts suppresses linear- and bridged-bonded CO on Rh^0 clusters and favors the formation of dicarbonyls as detected for sample 1.

Spectra recorded for Rh/TiO_2 samples, which are not reported here, showed adsorbate structures in between these two extremes illustrated in Fig. 4. As a possible explanation for the different CO dissociation capacity on various Rh/TiO_2 samples, a surface heterogeneity having more or less active sites for CO dissociation may be imagined.

General aspects of CO adsorption on differently supported rhodium. The band positions for CO adsorption on supported rhodium catalysts at 296 K and their assignments are listed in Table 1. Besides linear-bonded (2060–2075 cm^{-1}) and bridged-bonded CO (1810–1890 cm^{-1}), dicarbonyls (2090–2100 cm^{-1} and 2020–2035 cm^{-1}) were observed on supported rhodium. For catalysts with the same loading, a support effect in the formation of the different CO surface species became apparent: in accordance with literature data (16–18), dicarbonyls were strongly favored on Rh/Al_2O_3 compared to Rh/SiO_2. The fact, however, that these species were also dominant on Rh/TiO_2 is in contrast with conclusions given by Buchanan *et al.* (6). Applying the reasoning of the literature (16–18), it was therefore proven that oxidation potentials of OH groups to produce Rh^+ ions, which bind the dicarbonyl, should be identical for TiO_2 and Al_2O_3. Since dicarbonyls correspond to the dispersed phase, and linear- and bridged-bonded CO to crystalline rhodium, an increased number of small clusters has to be inferred when Al_2O_3 or TiO_2 instead of SiO_2 is used for catalyst preparation. As to the discrepancy which exists with results obtained by H_2 chemisorption (19), showing the highest H : Rh ratio for Rh/SiO_2 (see Table 1), one has to consider that the dispersed Rh^+ clusters are generated through CO adsorption (oxidative disruption).

Spectral evidence has been found that CO dissociates on Rh/Al_2O_3 and Rh/TiO_2, while CO adsorption at 296 K is nondissociative on Rh/SiO_2, as implied by the presence or absence of bands for oxidized rhodium, i.e., bands above 2100 cm^{-1}. Different intensities of such bands on various Rh/TiO_2 samples were explained by surface heterogeneity. There has been a dispute in the literature as to whether or not CO dissociates at ca. 300 K on supported rhodium. While Solymosi and Erdöhelyi (23, 24) reported that CO dissociation starts at ≥473 K only, Gélin *et al.* (5) demonstrated that CO is decomposed on a Rh(1.5 wt%)/NaY-zeolite catalyst at ≤300 K.

The different oxidation states on various Rh/TiO_2 samples as well as the support effect for $Rh^{>1+}$ also imply that oxygen contaminations of the N_2 gas cannot be regarded as a source for oxidized rhodium, since bands above 2100 cm^{-1} should then have been observed in every case. In addition, oxygen impurities can be excluded on the grounds that CO spectra recorded for catalysts which had been purged in flowing N_2 at 296 K overnight before adsorption runs were performed did not show any increase in intensity of bands for $Rh^{>1+}$, while even traces of oxygen should have led to such an increase.

From the results presented above, one may further conclude that CO dissociation has to be withdrawn as a possible driving force for producing Rh^+; bands for $Rh^{>1+}$ did not appear on Rh/SiO_2 and could not be detected on all Rh/TiO_2 samples although dicarbonyls were formed. It is

TABLE 1
Band Positions (in cm^{-1}) of Chemisorbed CO Species Detected on Supported Rh (0.5 wt%) Catalysts at 296 K

Catalysts	H:Rh[a]	ORhCO		ν_s $Rh(CO)_2$	RhCO	ν_{as} $Rh(CO)_2$	Rh_2CO	
		Rh^{3+}	Rh^{2+}	Rh^+	Rh^0	Rh^+	Rh^+	Rh^0
Rh/SiO_2	1.29			2097	2058 → 2065	2030		≈1830 → 1890
Rh/Al_2O_3	1.00		2120	2091		2020		≈1810 → 1835
Rh/TiO_2 (sample 1)	0.70	2145[b]	2135	2097 → 2100		2030 → 2034	2017[b]	≈1830
Rh/TiO_2 (sample 2)				2100	2075[b]	2036		≈1830

[a] H:Rh values exceeding unity may be explained by multiple adsorption or by hydrogen spillover from the metal to the support.
[b] Not observed at complete CO chemisorption.

therefore suggested that surface OH groups on different supports may play the dominant role in the oxidative disruption of Rh^0 clusters, as widely proposed in earlier studies (6–12).

2. CO Desorption at 296 K

Rh/SiO_2. When Rh/SiO_2 which had been previously exposed to CO was purged at 296 K with N_2, the desorption was complete after 3 h (see Fig. 5). During their loss in intensity, the dicarbonyl bands stayed constant in position at 2097 and 2030 cm^{-1}. The bands of linear- and bridged-bonded CO on Rh^0 shifted to lower wavenumbers, viz. 2065 → 2051 cm^{-1} and 1890 → 1830 cm^{-1}, respectively, due to weaker dipolar coupling of adsorbed CO molecules.

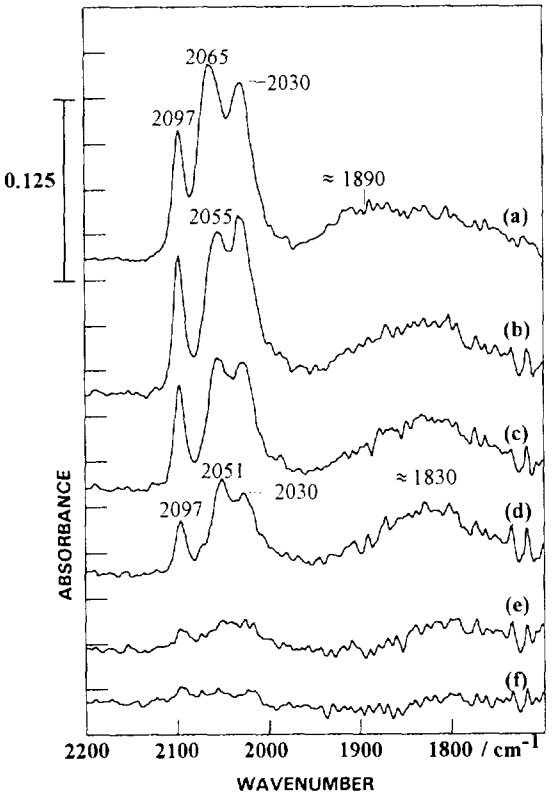

FIG. 5. Infrared spectra of CO adsorbed on Rh(0.5 wt%)/SiO_2: (a) complete CO chemisorption at 296 K; (b) flow of N_2 (10 cm^3 min^{-1}) for 0.5 h, (c) 1 h, (d) 1.5 h, (e) 2 h, and (f) 2.5 h.

Rh/Al_2O_3. A minor decrease of the strong dicarbonyl bands (2091 and 2020 cm^{-1}) and of the broad absorption of bridged-bonded CO on Rh^0 (1835 → 1815 cm^{-1}) was obtained after 13.5 h (see Fig. 6). While the abovementioned bands declined, the band at 2120 cm^{-1} of linear-bonded CO on Rh^{2+} increased in intensity. It is concluded that CO dissociates during desorption at 296 K. A Rh–O species obviously keeps CO more strongly bonded than the other adsorption sites.

Rh/TiO_2. Only very weak bands of the dicarbonyls (2100 and 2034 cm^{-1}) as well as of bridged-bonded CO on Rh^0 at ca. 1820 cm^{-1} (not shown in Fig. 7) remained on Rh/TiO_2 when the catalyst was purged with N_2 at 296 K for 10 h. The band at 2135 cm^{-1} had strongly increased in intensity and a new absorption appeared at 2145 cm^{-1}. The frequencies above 2100 cm^{-1} which belong to linear-bonded CO on Rh^{2+} and Rh^{3+}, respectively, again imply CO dissociation at 296 K. The band at 2017 cm^{-1} which developed during CO desorption is assigned to bridged-bonded CO on Rh^+.

General aspects of CO desorption at 296 K. As a common spectral feature for CO desorption at 296 K from the Rh/Al_2O_3 and Rh/TiO_2 catalyst a decline in band intensities of the dicarbonyl complex and of bridged-bonded CO on Rh^0 (linear-bonded CO on Rh^0 was not observed) which is accompanied by an increase or development of bands for oxidized rhodium, i.e., bands above 2100 cm^{-1}, may be mentioned. This is in contrast to results for Rh/SiO_2, which exhibits no new absorptions during CO desorption at 296 K. It is therefore concluded that CO dissociates on Rh/Al_2O_3 and Rh/TiO_2, while CO was not decomposed at 296 K in the case of Rh/SiO_2. Thus,

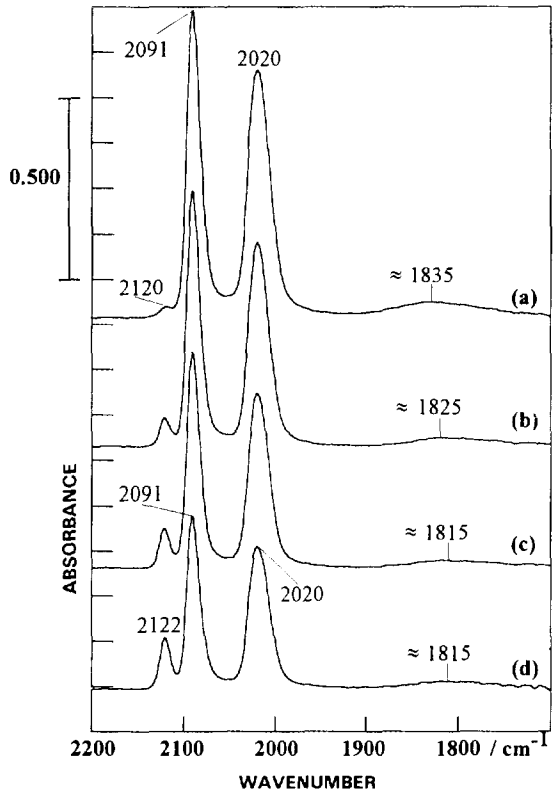

FIG. 6. Infrared spectra of CO adsorbed on Rh(0.5 wt%)/Al_2O_3: (a) complete CO chemisorption at 296 K; (b) flow of N_2 (10 cm^3 min^{-1}) for 4.5 h, (c) 7.5 h, and (d) 13.5 h.

by analogy with findings for CO adsorption, a support effect or a particle size effect again became evident since CO dissociation was detected on catalysts showing dicarbonyls as dominant surface species, i.e., there was a large extent of small Rh^+ clusters. The infrared results are also in agreement with CO-TPD studies (19, 25) performed on the same rhodium catalysts; CO dissociation was found for Rh/Al_2O_3 and Rh/TiO_2 only.

For the differently supported rhodium catalysts the rate of CO desorption at 296 K obeys the ensuing order: $Rh/SiO_2 > Rh/TiO_2 > Rh/Al_2O_3$. This is to say that adsorbed CO species were most stable on Rh/Al_2O_3. The desorption sequence corresponds to linear- and bridged-bonded CO on Rh^0 and to dicarbonyls on Rh^+; from the oxidized surface (bands above 2100 cm^{-1} for $Rh^{>1+}$), CO did not desorb at 296 K (the formation of the dicarbonyls is not attributed to the presence of oxygen).

3. Thermal CO Desorption

Rh/Al_2O_3. When the temperature was increased stepwise (25-K steps) on Rh/Al_2O_3 which had been previously exposed to CO at 296 K, a loss in band intensities of the dicarbonyl complex (2091 and 2020 cm^{-1}) and of bridged-bonded CO on Rh^0 (1835 → 1820 cm^{-1}) was first noted at 373 K (see Fig. 8). The band at 2120 cm^{-1} increased slightly, which implies that again a part of the CO dissociates. Above 373 K the dicarbonyl bands declined progressively slowly, until at 473 K a very strong decrease in intensity was obvious. At the same temperature a shoulder became visible at 1955 cm^{-1}; from this position, the presence of bridged-bonded CO on Rh^+ is proposed. Between 373 and 473 K, the band at 2120 cm^{-1} stayed constant but became then weaker at 498 K. While dicarbonyls and bridged-bonded CO species on Rh^0 had disappeared at 498 K, a new weak absorption was now apparent at ca. 2060 cm^{-1} which is due to linear-bonded CO on Rh^0; above 523 K, CO desorption was complete.

Rh/TiO_2. Applying the same procedure as described above, a strong decrease in intensity of the dicarbonyl bands (2100 and 2034 cm^{-1}) was observed at 398 K; linear-bonded CO species on Rh^{2+} (2135 cm^{-1}) had disappeared (see Fig. 9). The band of bridged-bonded CO on Rh^0 (ca. 1825 cm^{-1}), however, had increased in intensity and a new absorption of linear-bonded CO on Rh^0 developed at 2063 cm^{-1}. This may be interpreted by assuming that CO from the dicarbonyl complex is transformed to linear- and

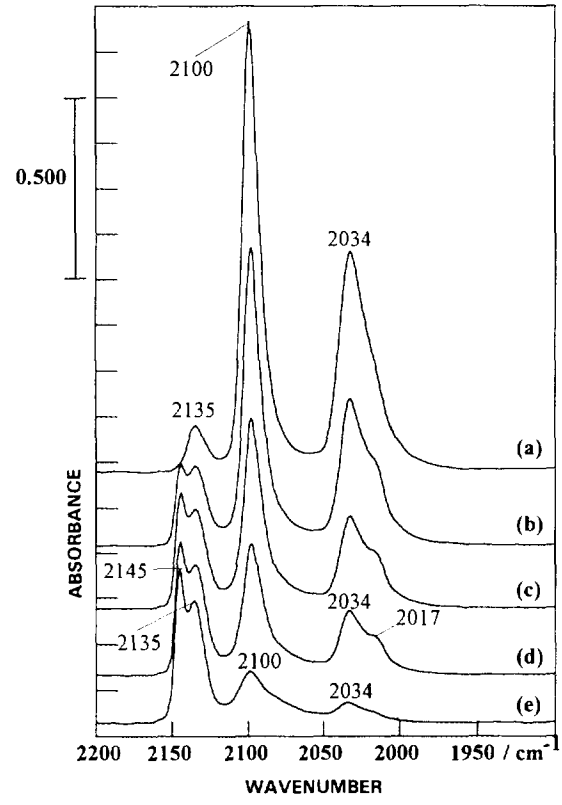

FIG. 7. Infrared spectra of CO adsorbed on Rh(0.5 wt%)/TiO_2: (a) complete CO chemisorption at 296 K; (b) flow of N_2 (10 cm^3 min^{-1}) for 1.25 h, (c) 2.5 h, (d) 3.75 h, and (e) 10 h.

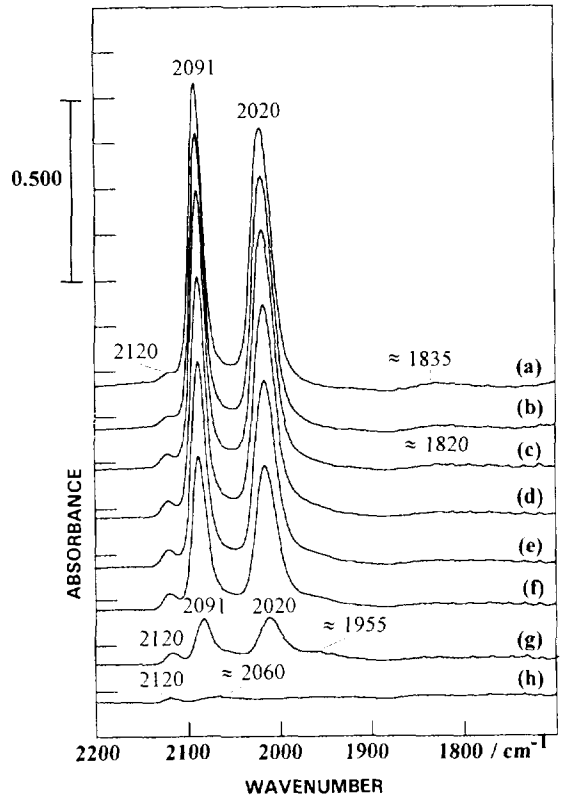

FIG. 8. Infrared spectra of CO adsorbed on *Rh*(0.5 wt%)/Al_2O_3: (a) complete CO chemisorption at 296 K; (b) heating in a flow of N_2 (10 cm^3 min^{-1}) to 348 K, (c) 373 K, (d) 398 K, (e) 423 K, (f) 448 K, (g) 473 K, and (h) 498 K.

bridged-bonded CO surface species. A new shoulder at ca. 2005 cm^{-1} is assigned to bridged-bonded CO on Rh^+. While at 423 K only a weak absorption of the dicarbonyl complex remained at 2096 cm^{-1}, absorptions of linear- and bridged-bonded CO on Rh^0 were well pronounced (2039 and ca. 1825 cm^{-1}, respectively). At 498 K, linear-bonded CO on Rh^0 was still seen at 2022 cm^{-1}; at 523 K, adsorbed CO surface species were completely removed.

General aspects of thermal CO desorption. In thermal CO desorption for Rh/Al_2O_3 and Rh/TiO_2 it became evident that initially formed dicarbonyls are transformed to linear- and bridged-bonded CO on Rh^0; this was more marked for Rh/TiO_2 than for Rh/Al_2O_3. The phenomenon, observed in the past for Rh/SiO_2 and Rh/Al_2O_3 only, had been ascribed to a reductive agglomeration of Rh^+ clusters induced by CO at higher temperatures (7, 15, 26–29) which is the reverse of the oxidative disruption of Rh^0 crystallites which occurs during CO adsorption at lower temperatures (ca. 300 K).

In contrast to the findings for desorption studies at 296 K, CO dissociation was just manifested on Rh/Al_2O_3 by a slight increase of the band of linear-bonded CO on Rh^{2+} at 2120 cm^{-1}. Obviously, at higher temperatures adsorbed oxygen reacts to form CO_2.

4. CO Re-adsorption

4.1. Re-adsorption after CO Desorption at 296 K

When Rh/Al_2O_3 and Rh/TiO_2 previously exposed to CO were purged in flowing N_2 at 296 K to investigate CO desorption, adsorbate structures as illustrated in Figs. 6 and 7 were obtained after ca. 15 h. For removal of these surface species the continuous flow was switched to H_2 (maximum 3 h) at 296 K. The catalysts were then purged again with N_2, and new CO adsorption runs were performed at 296 K for elucidating structural changes which may have occurred during CO desorption.

Rh/Al_2O_3. In comparison to the original spectrum of Rh/Al_2O_3, the spectra recorded after re-exposure to CO differed essentially (Fig. 10). Thus, in re-adsorption dicarbonyl bands at 2091 and 2020 cm^{-1} showed much lower intensities, while the band of bridged-bonded CO on Rh^0 had increased strongly and had shifted from 1835 to 1850 cm^{-1}. In addition, a new band of linear-bonded CO on

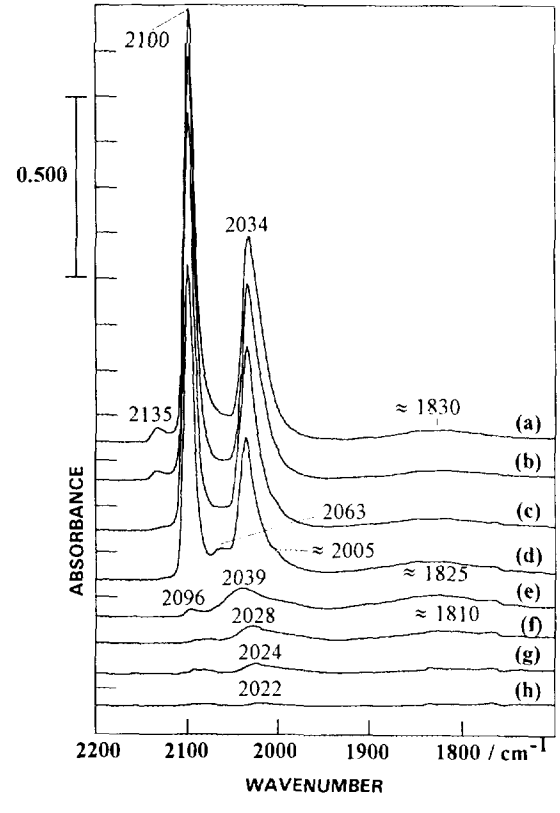

FIG. 9. Infrared spectra of CO adsorbed on Rh(0.5 wt%)/TiO_2: (a) complete CO chemisorption at 296 K; (b) heating in a flow of N_2 (10 cm^3 min^{-1}) to 348 K, (c) 373 K, (d) 398 K, (e) 423 K, (f) 448 K, (g) 473 K, and (h) 498 K.

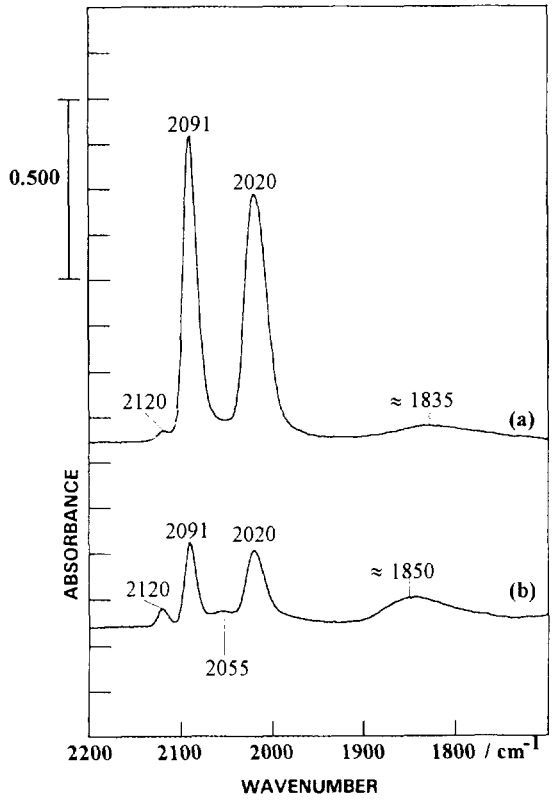

FIG. 10. Infrared spectra of CO adsorbed on Rh(0.5 wt%)/Al_2O_3: (a) complete CO chemisorption on the original reduced catalyst at 296 K and (b) re-adsorption after CO desorption at 296 K.

Rh^0 appeared at 2055 cm^{-1}. The increase of bands due to linear- and bridged-bonded CO on Rh^0 while the dicarbonyl bands strongly lost intensity demonstrates that structural changes, i.e., agglomeration of Rh^+ clusters, already starts during CO desorption at 296 K. The band at 2120 cm^{-1}, however, remained after prolonged H_2 treatment at 296 K (see above).

Rh/TiO₂. Similar to Rh/Al_2O_3, re-adsorption of CO led to significantly lower intensities of the dicarbonyl bands (see Fig. 11) compared to spectra originally detected on Rh/TiO_2 (Figs. 3 or 4). The band positions, however, were found at somewhat lower wavenumbers, viz., 2100 → 2096 cm^{-1} and 2035 → 2024 cm^{-1}, respectively. For low CO frequency values of the dicarbonyl bands, superpositions with absorptions due to linear- and bridged-bonded CO on Rh^+ have been suggested (see Section 1). The band of bridged-bonded CO on Rh^0 was much stronger in re-adsorption and had shifted from 1830 to 1870 cm^{-1}; linear-bonded CO on Rh^0 was now visible at 2051 cm^{-1}. From the band at 2131 cm^{-1}, again CO dissociation may be concluded.

4.2. Thermal CO Desorption

Figure 11 further shows results obtained for thermal CO desorption after re-adsorption on Rh/TiO_2, since the sequence of the disappearing surface species was then well identified. At 373 K, a very weak dicarbonyl band remained at 2096 cm^{-1}, linear-bonded CO on Rh^{2+} (2130–2135 cm^{-1}) had disappeared. The development of a band at 2017 cm^{-1}, which is ascribed to bridged-bonded CO on Rh^+, now explains the low CO frequency value of the dicarbonyl band at 296 K, i.e., at 2024 cm^{-1}, by their superposition. At 423 K, the only spectral feature consisted of strong and broad absorptions of linear- and bridged-bonded CO on Rh^0 (2043 and ca. 1850 cm^{-1}, respectively). At 523 K, a weak band of linear-bonded CO on Rh^0 was still seen at 2028 cm^{-1}, while at 548 K, CO desorption was complete.

The desorption sequence thus observed for the different CO surface species on supported rhodium followed the order $Rh(CO)_2 > Rh_2CO > RhCO$, which confirms earlier results of Yang and Garland (1).

4.3. Re-adsorption after Thermal CO Desorption

When CO desorbed from the Rh/Al_2O_3 and Rh/TiO_2 catalyst at higher temperatures (≥500 K), a re-exposure to CO at 296 K led again to weak dicarbonyl bands and to strong absorptions of linear- and bridged-bonded CO on Rh^0. An enormous enhancement in agglomeration of Rh^+ clusters, however, became evident, since overall integrated band areas reached only 30% of those calculated in re-adsorption after CO desorption at 296 K (Figs. 10 and 11).

Different catalyst treatments which were then performed, i.e., H_2 and O_2 treatments at 296 or 473 K, failed to reproduce the original adsorbate structures independently of whether readsorption had been carried out after isothermal (296 K) or thermal CO desorption.

General aspects of CO re-adsorption. Compared to the original reduced Rh/Al_2O_3 and Rh/TiO_2 catalyst, in re-adsorption of CO the formation of dicarbonyls was suppressed, linear-bonded (development of a new absorption at 2050–2055 cm^{-1}) and bridged-bonded CO species on Rh^0 were strongly favored. This corresponds to the reductive agglomeration process previously detected in thermal desorption (see Section 3); i.e., small Rh^+ clusters were reduced during their sintering. Band shifts of bridged-bonded CO on Rh^0 to higher wavenumbers (ca. 1835 → 1850 cm^{-1} and 1830 → 1870 cm^{-1}) also agree with the particle growth, since higher local density of adsorbed CO molecules on larger clusters results in stronger dipolar coupling. In contrast to the literature (7, 15, 26–29) where agglomeration of rhodium catalysts was reported for ≥473 K only, it has been proven that this phenomenon is already

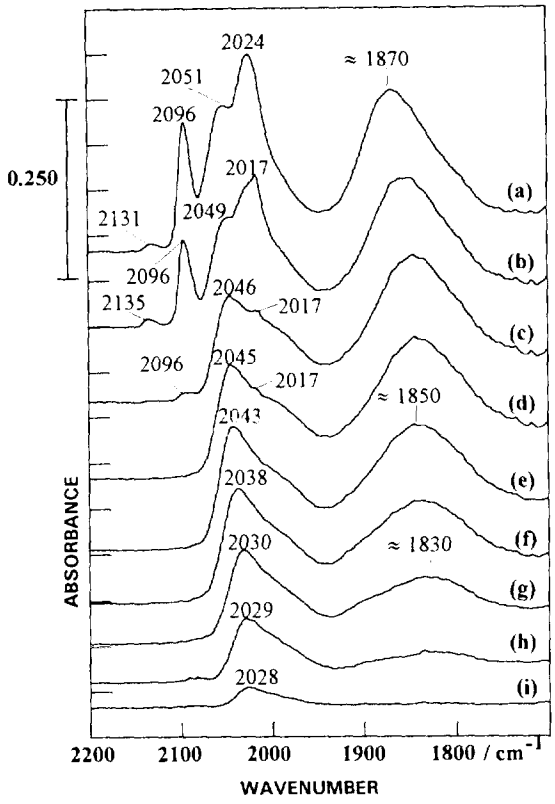

FIG. 11. Infrared spectra of CO adsorbed on Rh(0.5 wt%)/TiO_2: (a) re-adsorption after CO desorption at 296 K; (b) heating in a flow of N_2 (10 cm^3 min^{-1}) to 323 K, (c) 348 K, (d) 373 K, (e) 398 K, (f) 423 K, (g) 448 K, (h) 473 K, and (i) 498 K.

induced by CO desorption at 296 K which is then enhanced at higher temperatures; when overall integrated band areas are considered, the CO uptake did not exceed 30% of catalysts reconstructed at 296 K. The agglomeration, i.e., sintering, of Rh catalysts was irreversible, as already known from the literature (15).

CONCLUSIONS

On supported Rh (0.5 wt%) linear-bonded (2050–2075 cm^{-1}) and bridged-bonded CO (ca. 1810–1890 cm^{-1}) on crystalline Rh^0, as well as dicarbonyls on dispersed Rh^+ sites (2090–2100 cm^{-1} and 2020–2035 cm^{-1}), were generated. While the former surface species were well pronounced on Rh/SiO_2, dicarbonyls were dominant on Rh/Al_2O_3 and Rh/TiO_2. An increased number of small clusters was therefore discernable when Al_2O_3 or TiO_2 instead of SiO_2 were used in catalyst preparation. Additionally, similar oxidation potentials of OH groups on Al_2O_3 and TiO_2 to produce Rh^+ (oxidative disruption) may be drawn from these findings. The support and the particle size distribution influenced further adsorption and desorption behavior of CO: in contrast to Rh/SiO_2, CO was found to dissociate on Rh/Al_2O_3 and Rh/TiO_2 at 296 K, which was apparent by the presence or absence of bands for oxidized rhodium, i.e., bands above 2100 cm^{-1} for $Rh^{>1+}$. The support effect for $Rh^{>1+}$ in CO adsorption runs also demonstrated that CO dissociation cannot be regarded as the driving force for oxidative disruption of Rh^0 crystallites since dicarbonyls were observed independently. The CO desorption sequence occurred in the following orders: $Rh(CO)_2 > Rh_2CO > RhCO$ and Rh/SiO_2 > Rh/TiO_2 > Rh/Al_2O_3. This is to say that linear-bonded species on Rh^0 were most stable and CO was most strongly held on Rh/Al_2O_3. From the oxidized surface (bands above 2100 cm^{-1}), CO did not desorb at 296 K, while at higher temperatures adsorbed oxygen reacted to CO_2. In thermal CO desorption initially formed dicarbonyls were transformed to linear- and bridged-bonded CO on Rh^0, which was due to the reductive agglomeration, i.e., sintering, of Rh^+ clusters as described in the literature for ≥ 473 K (5, 15, 26–29). Re-adsorption studies proved that this phenomenon was already induced through CO desorption at 296 K, which was then only strongly enhanced when CO desorbed at higher temperatures (up to 500 K). In accordance with the literature (15), the agglomeration, i.e., sintering, of rhodium catalysts was irreversible. Especially, the IR results presented for Rh/TiO_2 were helpful for eluciating the role of the TiO_2 carrier in CO adsorption and desorption on highly dispersed rhodium which resembled the behavior of the Al_2O_3 support.

ACKNOWLEDGMENTS

The catalysts used in this study were kindly provided by Professor X. E. Verykios, Patras, Greece. Support of this work by the Deutsche Forschungsgemeinschaft is gratefully recognized.

REFERENCES

1. Yang, A. C., and Garland, C. W., *J. Phys. Chem.* **61,** 1504 (1957).
2. van't Blik, H. F. J., van Zon, J. B. A. D., Huizinga, T., Vis, J. C., Koningsberger, D. C., and Prins, R., *J. Phys. Chem.* **87,** 2264 (1983).
3. Primet, M., *J. Chem. Soc. Faraday Trans. 1* **74,** 2570 (1978).
4. Bergeret, G., Gallezot, P., Gélin, P., Ben Taarit, Y., Lefebvre, F., Naccache, C., and Shannon, R. D., *J. Catal.* **104,** 279 (1987).
5. Gélin, P., Dutel, J. F., and Ben Taarit, Y., *J. Chem. Soc. Chem. Commun.*, 1746 (1990).
6. Buchanan, D. A., Hernandez, M. E., Solymosi, F., and White, J. M., *J. Catal.* **125,** 456 (1990).
7. Solymosi, F., and Pásztor, M., *J. Phys. Chem.* **89,** 4783 (1985).
8. Solymosi, F., and Pásztor, M., *J. Phys. Chem.* **90,** 5312 (1986).
9. Basu, P., Panayotov, D., and Yates, J. T., *J. Phys. Chem.* **91,** 3133 (1987).
10. Smith, A. K., Hagues, F., Theolier, A., Basset, J. M. Ugo, R., Zanderighi, G. M., Bilhou, J. L., Bilhou-Bougnol, V., and Graydon, W. F., *Inorg. Chem.* **18,** 3104 (1979).
11. Theshir, A., Smith, A. K. Lecomte, M. S., Basset, J. M., Zanderighi, G. M., Psaro, R., and Ugo, R., *J. Organomet. Chem.* **191,** 415 (1980).

12. Bilhou, J. L., Bilhou-Bougnol, V., Graydon, W. F., Basset, J. M., Smith, A. K., Zanderighi, G. M., and Ugo, R. *J. Organomet. Chem.* **153,** 73 (1978).
13. van't Blik, H. F. J., van Zon, J. B. A. D., Huizinga, T., Vis, J. C., Koningsberger, D. C., and Prins, R., *J. Am. Chem. Soc.* **107,** 3139 (1985).
14. van't Blik, H. F. J., van Zon, J. B. A. D., Huizinga, T., Vis, J. C. Koningsberger, D. C., and Prins, R., *J. Mol. Catal.* **25,** 379 (1984).
15. Solymosi, F., and Knözinger, H., *J. Chem. Soc. Faraday Trans.* **86,** 389 (1990).
16. Solymosi, F., Pásztor, M., and Rákhely, G., *J. Catal.* **110,** 413 (1988).
17. Zaki, M. I., Tesche, B., Kraus, L., and Knözinger, H., *Surf. Interface Anal.* **12,** 239 (1988).
18. McQuire, M. W., McQuire, G. W., and Rochester, C. H., *J. Chem. Soc. Faraday Trans.* **88,** 1203 (1992).
19. Ioannides, T., and Verykios, X. E., *J. Catal.* **140,** 353 (1993).
20. Wey, J. P., Neely, W. C., and Worley, S. D., *J. Catal.* **134,** 378 (1992).
21. Rice, C. A., Worley, S. D., Curtis, C. W., Guin, J. A., and Tarrer, A. R., *J. Chem. Phys.* **74,** 6487 (1981).
22. Cavanagh, R. R., and Yates, J. T., *J. Chem. Phys.* **74,** 4150 (1981).
23. Solymosi, F., and Erdöhelyi, A., *Surf. Sci.* **110,** 1630 (1981).
24. Erdöhelyi, A., and Solymosi, F., *J. Catal.* **84,** 446 (1983).
25. Dropsch, H., and Baerns, M., unpublished.
26. Dictor, R., and Roberts, S., *J. Phys. Chem.* **93,** 2526 (1989).
27. Dictor, R., and Roberts, S., *J. Phys. Chem.* **93,** 5846 (1989).
28. Anderson, J. A., and Rochester, C. H., *J. Chem. Soc. Faraday Trans.* **87,** 1479 (1991).
29. Anderson, J. A., *J. Chem. Soc. Faraday Trans.* **87,** 3907 (1991).